Fermi National Accelerator Laboratory

FERMILAB-Pub-92/167-E

A Measurement of Jet Shapes in $p\bar{p}$ Collisions at $\sqrt{s} = 1.8$ TeV

The CDF Collaboration

Fermi National Accelerator Laboratory, Batavia, Illinois 60510

June 1992

Submitted to *Physical Review Letters*

Operated by Universities Research Association Inc. under Contract No. DE-AC02-76CHO3000 with the United States Department of Energy

Disclaimer

CDF/PUB/JET/PUBLIC/1708
FERMILAB-PUB-92/167-E

A Measurement of Jet Shapes in $\bar{p}p$ Collisions at $\sqrt{s} = 1.8$ TeV

F. Abe,[11] D. Amidei,[14] C. Anway-Weiss,[3] G. Apollinari,[20] M. Atac,[6] P. Auchincloss,[19]
A. R. Baden,[8] N. Bacchetta,[15] W. Badgett,[14] M. W. Bailey,[18] A. Bamberger,[6,a]
P. de Barbaro,[19] A. Barbaro-Galtieri,[12] V. E. Barnes,[18] B. A. Barnett,[10] G. Bauer,[13]
T. Baumann,[8] F. Bedeschi,[17] S. Behrends,[2] S. Belforte,[17] G. Bellettini,[17] J. Bellinger,[25]
D. Benjamin,[24] J. Benlloch,[6,a] J. Bensinger,[2] A. Beretvas,[6] J. P. Berge,[6] S. Bertolucci,[7]
S. Bhadra,[9] M. Binkley,[6] D. Bisello,[15] R. Blair,[1] C. Blocker,[2] A. Bodek,[19] V. Bolognesi,[17]
A. W. Booth,[6] C. Boswell,[10] G. Brandenburg,[8] D. Brown,[8] E. Buckley-Geer,[21] H. S. Budd,[19]
G. Busetto,[15] A. Byon-Wagner,[6] K. L. Byrum,[25] C. Campagnari,[6] M. Campbell,[14]
A. Caner,[6] R. Carey,[8] W. Carithers,[12] D. Carlsmith,[25] J. T. Carroll,[6] R. Cashmore,[6,a]
A. Castro,[15] F. Cervelli,[17] K. Chadwick,[6] J. Chapman,[14] G. Chiarelli,[7] W. Chinowsky,[12]
S. Cihangir,[6] A. G. Clark,[6] M. Cobal,[17] D. Connor,[16] M. Contreras,[4] J. Cooper,[6]
M. Cordelli,[7] D. Crane,[6] J. D. Cunningham,[2] C. Day,[6] F. DeJongh,[6] S. Dell'Agnello,[17]
M. Dell'Orso,[17] L. Demortier,[2] B. Denby,[6] P. F. Derwent,[14] T. Devlin,[21] D. DiBitonto,[22]
M. Dickson,[20] R. B. Drucker,[12] K. Einsweiler,[12] J. E. Elias,[6] R. Ely,[12] S. Eno,[4]
S. Errede,[9] A. Etchegoyen,[6,a] B. Farhat,[13] B. Flaugher,[6] G. W. Foster,[6] M. Franklin,[8]
J. Freeman,[6] H. Frisch,[4] T. Fuess,[6] Y. Fukui,[11] A. F. Garfinkel,[18] A. Gauthier,[9]
S. Geer,[6] D. W. Gerdes,[4] P. Giannetti,[17] N. Giokaris,[20] P. Giromini,[7] L. Gladney,[16]
M. Gold,[12] K. Goulianos,[20] H. Grassmann,[15] G. M. Grieco,[17] C. Grosso-Pilcher,[4]
C. Haber,[12] S. R. Hahn,[6] R. Handler,[25] K. Hara,[23] B. Harral,[16] R. M. Harris,[6]
S. A. Hauger,[5] J. Hauser,[3] C. Hawk,[21] T. Hessing,[22] R. Hollebeek,[16] L. Holloway,[9]
S. Hong,[14] P. Hu,[21] B. Hubbard,[12] B. T. Huffman,[18] R. Hughes,[16] P. Hurst,[8]

Submitted to Physical Review Letters, June 12, 1992

J. Huth,[6] J. Hylen,[6] M. Incagli,[17] T. Ino,[23] H. Iso,[23] H. Jensen,[6] C. P. Jessop,[8] R. P. Johnson,[6] U. Joshi,[6] R. W. Kadel,[12] T. Kamon,[22] S. Kanda,[23] D. A. Kardelis,[9] I. Karliner,[9] E. Kearns,[8] L. Keeble,[22] R. Kephart,[6] P. Kesten,[2] R. M. Keup,[9] H. Keutelian,[6] D. Kim,[6] S. B. Kim,[14] S. H. Kim,[23] Y. K. Kim,[12] L. Kirsch,[2] K. Kondo,[23] J. Konigsberg,[8] E. Kovacs,[6] M. Krasberg,[14] S. E. Kuhlmann,[1] E. Kuns,[21] A. T. Laasanen,[18] S. Lammel,[3] J. I. Lamoureux,[25] S. Leone,[17] J. D. Lewis,[6] W. Li,[1] P. Limon,[6] M. Lindgren,[3] T. M. Liss,[9] N. Lockyer,[16] M. Loreti,[15] E. H. Low,[16] C. B. Luchini,[9] P. Lukens,[6] P. Maas,[25] K. Maeshima,[6] M. Mangano,[17] J. P. Marriner,[6] M. Mariotti,[17] R. Markeloff,[25] L. A. Markosky,[25] R. Mattingly,[2] P. McIntyre,[22] A. Menzione,[17] T. Meyer,[22] S. Mikamo,[11] M. Miller,[4] T. Mimashi,[23] S. Miscetti,[7] M. Mishina,[11] S. Miyashita,[23] Y. Morita,[23] S. Moulding,[2] J. Mueller,[21] A. Mukherjee,[6] T. Muller,[3] L. F. Nakae,[2] I. Nakano,[23] C. Nelson,[6] C. Newman-Holmes,[6] J. S. T. Ng,[8] M. Ninomiya,[23] L. Nodulman,[1] S. Ogawa,[23] R. Paoletti,[17] V. Papadimitriou,[6] A. Para,[6] E. Pare,[8] S. Park,[6] J. Patrick,[6] G. Pauletta,[17] L. Pescara,[15] T. J. Phillips,[5] F. Ptohos,[8] R. Plunkett,[6] L. Pondrom,[25] J. Proudfoot,[1] G. Punzi,[17] D. Quarrie,[6] K. Ragan,[16] G. Redlinger,[4] J. Rhoades,[25] M. Roach,[24] F. Rimondi,[6,a] L. Ristori,[17] W. J. Robertson,[5] T. Rodrigo,[6] T. Rohaly,[16] A. Roodman,[4] W. K. Sakumoto,[19] A. Sansoni,[7] R. D. Sard,[9] A. Savoy-Navarro,[6] V. Scarpine,[9] P. Schlabach,[8] E. E. Schmidt,[6] O. Schneider,[12] M. H. Schub,[18] R. Schwitters,[8] A. Scribano,[17] S. Segler,[6] Y. Seiya,[23] M. Shapiro,[12] N. M. Shaw,[18] M. Sheaff,[25] M. Shochet,[4] J. Siegrist,[12] P. Sinervo,[16] J. Skarha,[10] K. Sliwa,[24] D. A. Smith,[17] F. D. Snider,[10] L. Song, [6] T. Song,[14] M. Spahn,[12] P. Sphicas,[13] R. St. Denis,[8] A. Stefanini,[17] G. Sullivan,[4] K. Sumorok,[13] R. L. Swartz, Jr.,[9] M. Takano,[23] K. Takikawa,[23] S. Tarem,[2] F. Tartarelli,[17] S. Tether,[13] D. Theriot,[6] M. Timko,[24] P. Tipton,[19] S. Tkaczyk,[6] A. Tollestrup,[6] J. Tonnison,[18] W. Trischuk,[8] N. Turini,[17] Y. Tsay,[4] F. Ukegawa,[23] D. Underwood,[1] S. Vejcik, III,[10] R. Vidal,[6]

R. G. Wagner,[1] R. L. Wagner,[6] N. Wainer,[6] J. Walsh,[16] T. Watts,[21] R. Webb,[22] C. Wendt,[25] H. Wenzel,[17] W. C. Wester, III,[12] T. Westhusing,[9] S. N. White,[20] A. B. Wicklund,[1] E. Wicklund,[6] H. H. Williams,[16] B. L. Winer,[19] D. Wu,[14] J. Wyss,[15] A. Yagil,[6] K. Yasuoka,[23] G. P. Yeh,[6] J. Yoh,[6] M. Yokoyama,[23] J. C. Yun,[6] A. Zanetti,[17] F. Zetti,[17] S. Zhang,[14] S. Zucchelli,[6,a]

The CDF Collaboration

[1] *Argonne National Laboratory, Argonne, Illinois 60439*

[2] *Brandeis University, Waltham, Massachusetts 02254*

[3] *University of California at Los Angeles, Los Angeles, California 90024*

[4] *University of Chicago, Chicago, Illinois 60637*

[5] *Duke University, Durham, North Carolina 27706*

[6] *Fermi National Accelerator Laboratory, Batavia, Illinois 60510*

[7] *Laboratori Nazionali di Frascati, Istituto Nazionale di Fisica Nucleare, Frascati, Italy*

[8] *Harvard University, Cambridge, Massachusetts 02138*

[9] *University of Illinois, Urbana, Illinois 61801*

[10] *The Johns Hopkins University, Baltimore, Maryland 21218*

[11] *National Laboratory for High Energy Physics (KEK), Japan*

[12] *Lawrence Berkeley Laboratory, Berkeley, California 94720*

[13] *Massachusetts Institute of Technology, Cambridge, Massachusetts 02139*

[14] *University of Michigan, Ann Arbor, Michigan 48109*

[15] *Universita di Padova, Instituto Nazionale di Fisica Nucleare, Sezione di Padova, I-35131 Padova, Italy*

[16] *University of Pennsylvania, Philadelphia, Pennsylvania 19104*

[17] *Istituto Nazionale di Fisica Nucleare, University and Scuola Normale Superiore of Pisa, I-56100 Pisa, Italy*

[18] *Purdue University, West Lafayette, Indiana 47907*

(19) *University of Rochester, Rochester, New York 15627*

(20) *Rockefeller University, New York, New York 10021*

(21) *Rutgers University, Piscataway, New Jersey 08854*

(22) *Texas A&M University, College Station, Texas 77843*

(23) *University of Tsukuba, Tsukuba, Ibaraki 305, Japan*

(24) *Tufts University, Medford, Massachusetts 02155*

(25) *University of Wisconsin, Madison, Wisconsin 53706*

PACS. 12.38.Qk, 13.87.Ce

Abstract

We present a measurement of jet shapes in $\bar{\mathrm{p}}\mathrm{p}$ collisions at $\sqrt{\mathrm{s}} = 1.8$ TeV at the Fermilab Tevatron using the Collider Detector at Fermilab (CDF). Qualitative agreement is seen with the predictions of recent next-to-leading ($\mathcal{O}(\alpha_s^3)$) calculations and with leading logarithm QCD based Monte Carlos. The dependence of the jet shape on transverse energy is studied.

.....

In this letter we report an analysis of jet shapes, measured using the momentum flow of charged particles inside jets, and the dependence of the jet shape on jet energy for jets in the 100 GeV energy range. The experimental data, gathered using the CDF detector in $\bar{\mathrm{p}}\mathrm{p}$ collisions at $\sqrt{\mathrm{s}} = 1.8$ TeV, are compared to the calculation of Ellis et al. [1, 2] and leading logarithm QCD Monte Carlos [3, 4].

Such comparisons between QCD calculations and observations in jet physics have been plagued by a lack of knowledge of the fragmentation process. Although a large amount of experimental data has been accumulated on jet fragmentation, there are still no reliable techniques to calculate QCD in this soft regime. However, the main kinematic features of the non-perturbative hadronization process can be summarized by its longitudinal and lateral properties with respect to the jet axis: the longitudinal momentum (K_l) distribution approximately scales with jet energy, apart from logarithmic violations [5, 6, 7]; the transverse momentum (K_t) spectrum of the particles in the jet has a mean K_t of$\sim$ 350–500 MeV, which also changes slowly with jet energy [5, 8].

Based on the above, the mean angle δ between a particle and jet axis, where $\tan\delta = K_t/K_l$, should decrease with jet energy as K_t remains almost constant and K_l grows almost linearly with jet energy. Thus the size of a cone which contains a constant fraction of the the jet energy is expected to decrease with jet energy. At high energies, however, gluon emission effects are more prominent due to scaling of the matrix elements. Therefore, at sufficiently high energies where fragmentation effects become negligible, the shape of the jet should be calculable by perturbative QCD alone.

The Fermilab Tevatron has produced the most energetic jets ever seen. Therefore, it is interesting to test whether the shape of these jets, measured by momentum flow within a cone, can indeed be calculated by an α_s^3 finite-order perturbative QCD calculation [1]. Such a calculation has been shown to agree very well with the inclusive $d^2\sigma/dE_T d\eta$ jet cross section [9], where $E_T = E \cdot \sin\theta$, E is the jet energy,

$\eta \equiv -\log \tan(\theta/2)$ and θ is the polar angle with respect to the beam. Henceforth, transverse refers to the beam (i.e. $p\bar{p}$) axis.

The CDF detector has been described in detail elsewhere [10]. The detector elements most relevant to this study are the central calorimeter and the central tracking chamber. The calorimeter covers the pseudorapidity range $|\eta| \leq 1.1$. This calorimeter is segmented into projective towers of $\Delta\eta \times \Delta\phi = 0.1 \times 15^{\circ}$. Charged-particle momenta are measured with the central tracking chamber, a cylindrical drift chamber immersed in a 1.4 T solenoidal magnetic field parallel to the beam axis. In the pseudorapidity range $|\eta| < 1.2$, the transverse momentum resolution is $\delta P_T/P_T^2 \sim 0.002$ $(\mathrm{GeV/c})^{-1}$. The polar angle is measured with an accuracy $\delta \cot\theta$ of $\pm 5 \cdot 10^{-3}$. The detector was triggered on the presence of a localized cluster of energy in the calorimeter [11]. In order to span a large range of cross sections, three separate thresholds, of 20, 40, and 60 GeV, were imposed on the transverse energy of the trigger cluster. The 20 and 40 GeV triggers were prescaled to accept 1 in 300 and 1 in 30 events, respectively. The data set analyzed here corresponds to an integrated luminosity of 4.2 pb^{-1} at a center of mass energy $\sqrt{s} = 1.8$ TeV.

Jets are identified using a cone algorithm based on the measured event vertex as the origin. Contiguous seed towers with $E_T > 1$ GeV are selected to form preclusters. Using the E_T weighted centroid of each precluster as a starting point, jet clusters are formed by including all towers with $E_T > 0.1$ GeV inside a cone of radius $\mathrm{R_0} = \sqrt{(\Delta\eta)^2 + (\Delta\phi)^2}$ (ϕ measured in radians). A tower is included in a cluster if its center is inside the cone, otherwise it is excluded. A cone of $R_0 = 1.0$ is used in this analysis to minimize the flow of energy out of the jet cone. If a cluster shares more

than 75% of its energy with a cluster of higher energy, the two are merged together, otherwise, they are defined as separate, and towers common to both clusters are assigned to the jet with the nearest centroid. Further details on this algorithm can be obtained in Ref. [11]. The jet energy, E, is determined using a scalar sum of tower energies in the cone. E_T is measured as E $\sin\theta$, where θ is the angle between a line drawn from the cluster centroid to the event vertex position and the beamline. The jet axis used in the jet shape computation is defined by the following:

$$\eta_{jet} = \frac{\sum_{towers} \eta_i E_T}{\sum_{towers} E_T} \qquad \phi_{jet} = \frac{\sum_{towers} \phi_i E_T}{\sum_{towers} E_T} \tag{1}$$

The above algorithm is very similar to the jet definition employed at the parton level in producing the $\mathcal{O}(\alpha_s^3)$ predictions for comparison [1, 12].

Cuts were applied on the data to ensure uniform acceptance. The event vertex was required to be within 60 cm of the center of the detector along the beamline. A minimum energy cut, based on the trigger efficiency determined with jets in the region of E_T where the data from different triggers overlapped, was applied to avoid trigger biases. A maximum energy cut was also imposed to produce three non-overlapping samples for the study of the jet shape variation with energy. The obtained ranges were 40–60, 65–90, and 95–120 GeV, having mean energies of 45, 70 and 100 GeV, for the 20, 40 and 60 GeV triggers respectively. Background from cosmic ray showers were rejected using criteria based on timing information in the hadronic calorimeter and jet E_T balancing, similar to those described in Ref. [13]. Finally, jets in the sample were required to have $0.1 \leq |\eta| \leq 0.7$ to ensure uniform detector response and good containment in the central detector.

Tracks were used to study the jet shapes because of their better spatial and mo-

mentum resolution for single particles. The shape is defined by the normalized average transverse momentum (P_T) density $\rho(r)$:

$$\rho(r) = \frac{\xi(r)}{\int_0^{R_0} \xi(r)dr} \qquad \text{with} \qquad \xi(r) \equiv \frac{1}{\mathcal{N}_{jet}} \sum_{jets} \int_{P_T > P_T^{min}} \frac{P_T}{\mathcal{P}_T^{jet}} \frac{d^2N}{dr\,dP_T} dP_T \quad (2)$$

In these equations N is the number of tracks, P_T is their transverse momentum, $\mathcal{P}_T^{jet}$ is the total transverse momentum carried by tracks in the jet defined within a cone R_0, and r is the distance of the track from the jet axis in η-ϕ space ($r = \sqrt{(\Delta\eta)^2 + (\Delta\phi)^2}$). The minimum momentum measured by the central tracking chamber, P_T^{min}, is 0.4 GeV, and the cone size R_0 is selected to be 1.0. $\mathcal{N}_{jet}$ is the number of jets measured. The integral shape variable $\Psi(r) = \int_0^r \rho(r')dr'$ is used to compare data with theory. Note that r is related to the angle δ through the relation between η and θ: For small angles, $\Delta\eta = \Delta\theta/\sin\theta$ and $\delta = \sqrt{(\Delta\theta)^2 + (\Delta\phi)^2}$.

The theoretical predictions for the integral jet shape are obtained by calculating the phase space for two partons, weighted by their E_T and the appropriate matrix element squared, between the inner cone r and the jet cone R_0 [2]. The result is normalized by the total Born cross section. Assuming that non-perturbative effects do not change the jet shape substantially, this quantity is $1 - \Psi(r)$. This procedure is used in order to avoid collinear singularities at $r = 0$. We note that the α_S^3 theory does not predict substantial differences between quark and gluon jet shapes.

In Figure 1.a, the integrated jet shape Ψ is shown and compared with an α_s^3 calculation by S. Ellis, for three different renormalization scales μ [2], and with the result of the Herwig [3] Monte Carlo, which includes fragmentation effects. Non-perturbative effects are not added to the QCD curves. It is remarkable that a pure perturbative QCD calculation can describe the experimental data so well. A simple independent

jet fragmentation model without gluon radiation predicts a much narrower jet shape.

The measurement of the shape can be distorted by various experimental effects. The dominant ones are the spatial resolution of jet axis position and tracking inefficiency at the jet core. Both effects tend to smear energy out from the core to the adjacent regions.

The tracking efficiency in jets was estimated by merging drift chamber hits from simulated tracks into real jet data, as in Ref. [6]. Those events were tracked by the same algorithm used for real data, and the resulting efficiency was parametrized as a function of the spatial separation of tracks and the jet E_T. The parametrization was incorporated in the fast detector simulation used for this analysis. The systematic uncertainty in this procedure was estimated by comparing the jet shape distribution obtained by generating jet events and propagating them through two different detector simulations, one which uses the efficiency parametrization, and one which generates drift chamber hits which are subsequently tracked by the CDF tracking algorithm. The difference between these two distributions was used as the systematic uncertainty. This uncertainty varies between 6% for $r < 0.1$ to less than 1% for $r > 0.4$.

The uncertainty in the jet axis position introduces a correlation in r, found to be mainly between adjacent bins in r, in the measured distribution. For example if the resolution is Δr then a particle produced at distance r from the real jet axis may be detected at $r + \Delta r$ in a different bin. To unfold this effect, we use a correction matrix, calculated from a Monte Carlo simulation, in the following way. We determine the matrix $\mathcal{A}$, defined such that $\rho_{det} = \mathcal{A}\rho_{gen}$, where ρ_{det} is the jet shape distribution obtained from Monte Carlo detector simulation and and ρ_{gen} is the generated dis-

tribution. The elements of matrix $\mathcal{A}$ are found by summing over all contributions in a bin in the space (r_{det}, r_{gen}) and the matrix is then normalized by rows to fulfill $\rho_{det} = \mathcal{A}\rho_{gen}$. The inverse matrix $\mathcal{A}^{-1}$ is used to correct the data: $\rho_{corr} = \mathcal{A}^{-1}\rho_{meas}$, where ρ_{corr} is the corrected distribution and ρ_{meas} is the measured distribution. This procedure corrects also for known detector effects such as tracking efficiency, mentioned above. The correction is of the order of 6% for $r = 0.1$ and less than 3% for the other r bins.

The stability of the correction method was checked by the following procedure. Two correction matrices were generated with two different Monte Carlos, Herwig 5.3 [3] and Pythia 5.4 [4]. The correction matrix of the first was applied to the obtained distribution (after detector simulation) of the second and vice versa. The result of the matrix corrections was compared with the generated distributions. The difference between the corrected and generated distributions was added to the systematic uncertainty. They vary from 7% for $r < 0.1$ to less than 1% for $r > 0.3$.

The uncertainty from the jet axis definition was estimated by comparing the jet shape distributions from Monte Carlo generated events, using two different jet axes: the jet axis obtained from the CDF jet algorithm after the events were propagated through the detector simulation, and the jet axis obtained from clustering the generated particles. The uncertainty varies from 6% at $r < 0.1$ to 1% and less for $r > 0.2$. The systematic uncertainty from fragmentation was estimated by comparing the results of the Pythia Monte Carlo with the Herwig Monte Carlo. This uncertainty is less than 1% for all r.

Finally, underlying event contributions to the shape are small, as their shape is

flat and the energy small compared to the jet energies used. The calorimeter energy scale is uncertain to 3% and this leads to a systematic uncertainty in the jet shape measurement which varies from 4% for $r < 0.1$ to less than 1% for $r > 0.2$.

The total systematic uncertainty was estimated by adding all above sources in quadrature. The uncertainty is of the order of 10% for $r < 0.1$, decreasing with r to less than 1% for $r > 0.5$. The uncertainty is similar for the three jet energies studied.

In Figure 1.b, Ψ is plotted for the three different energies, 45, 70 and 100 GeV. One can observe that the jets get narrower as their E_T increases. In order to compare the data to theory and to QCD Monte Carlos, the energy dependence of the shape is shown in Figure 2 by plotting the fractional P_T inside of a typical cone of r=0.4, for the three different energies. Also plotted are the predictions of the Herwig and Pythia Monte Carlos, with their respective default structure functions, DO [14] and EHLQ [15], and the predictions of the α_s^3 theory, using HMRSB [16]. The bands represent the uncertainty in the α_s^3 theory due to the renormalization scale.

Both the α_s^3 theory and the leading log shower Monte Carlos, agree qualitatively with the data, although it seems that the jets are slightly more collimated than the α_s^3 theory and slightly less collimated than the prediction of the shower Monte Carlos. One possible explanation for the observation that high energy jets are narrower than the α_s^3 prediction is that higher order effects tend, through coherent gluon emission [17], to populate with soft partons the region between the 'hard' emission and the original parton, transferring some of the energy of the hard parton to the inner part of the jet.

In conclusion, it is encouraging that the calculation of the jet internal structure

by a perturbative expansion in α_S is so close to the experimental data. This might be the first step in understanding jet formation from first principles, without relying on phenomenological models.

We thank the Fermilab staff and the technical staffs of the participating institutions for their vital contributions. This work is supported by the U.S. Department of Energy and National Science Foundation; the Italian Istituto Nazionale di Fisica Nucleare; the Ministry of Science, Culture, and Education of Japan; and the A. P. Sloan Foundation. We also wish to thank S. Ellis for useful discussions and for providing results of his calculations.

References

[1] S.D. Ellis, Z. Kunszt and D.E. Soper, Phys. Rev. Lett. **64** (1990) 2121.

[2] S.D. Ellis, Z. Kunszt and D.E. Soper, UW/PT-91-13, Proc. of Lepton–Hadron Conf., Geneva, 1992 and UW/PT-92-01; S.D. Ellis, private communication.

[3] G. Marchesini and B.R. Webber, Nucl. Phys. B310 (1988) 461.

[4] H.U. Bengtsson, T. Sjostrand, Computer Phys. Comm. 46 (1987) 43; T. Sjostrand, Computer Phys. Comm. 39 (1986) 347.

[5] TASSO Coll., M. Althoff et al., Z. Phys **C22** (1984) 307.

[6] CDF Coll., F. Abe et al., Phys. Rev. Lett. **65** (1990) 968.

[7] MarkII Coll., G.S.Abrams et al., Phys. Rev. Lett. **64** (1990) 1334.

[8] Amy Coll., Y.K. Li et al., Phys. Rev. **D41** (1990) 2675.

[9] CDF Coll., F. Abe et al., Phys. Rev. Lett. **68** (1992) 1104.

[10] CDF Coll., F. Abe et al., Nucl. Instr. Meth. **A271** (1988) 387.

[11] CDF Coll., F. Abe et al., Phys. Rev. **D45** (1992) 1448.

[12] J. E. Huth et al., FERMILAB-CONF-90-249-E, Snowmass 1990.

[13] CDF Coll., F. Abe et al., Phys. Rev. Lett. **62** (1989) 613.

[14] D.W. Duke and J.F. Owens, Phys. Rev. **D30** (1984) 49.

[15] E. Eichten, I. Hinchliffe, K. Lane and C. Quigg, Rev. Mod. Phys. **56** (1984) 579.

[16] P. Harriman, A. Martin, R. Roberts and W. Stirling, Phys. Rev. **D42** (1990) 798.

[17] A. Bassetto, M. Ciafaloni and G. Marchesini, Phys. Rep. **100** (1983) 202.

Figure Captions

Fig. 1: a)The distribution of the P_T fraction in a cone for 100 GeV E_T jets and cone size of $R_0 = 1.0$. The variable plotted, $\Psi(r)$, is the ratio of P_T within a cone of radius r to the P_T within a cone of radius $R_0 = 1.0$. Also shown are QCD calculations: α_s^3 theory calculations, using HMRSB structure functions for $\Lambda_{QCD} = 122$ MeV and different scales μ; the prediction from the Herwig Monte Carlo version 5.3.

b) $\Psi(r)$ for 45, 70 and 100 GeV jets.

Fig. 2: $\Psi(0.4)$ for 45, 70 and 100 GeV jets. The horizontal error bars represent the jets E_T range. Predictions from the α_s^3 theory (the width of the band represents the μ dependence) and the Herwig and Pythia Monte Carlos are also shown.

Figure 1

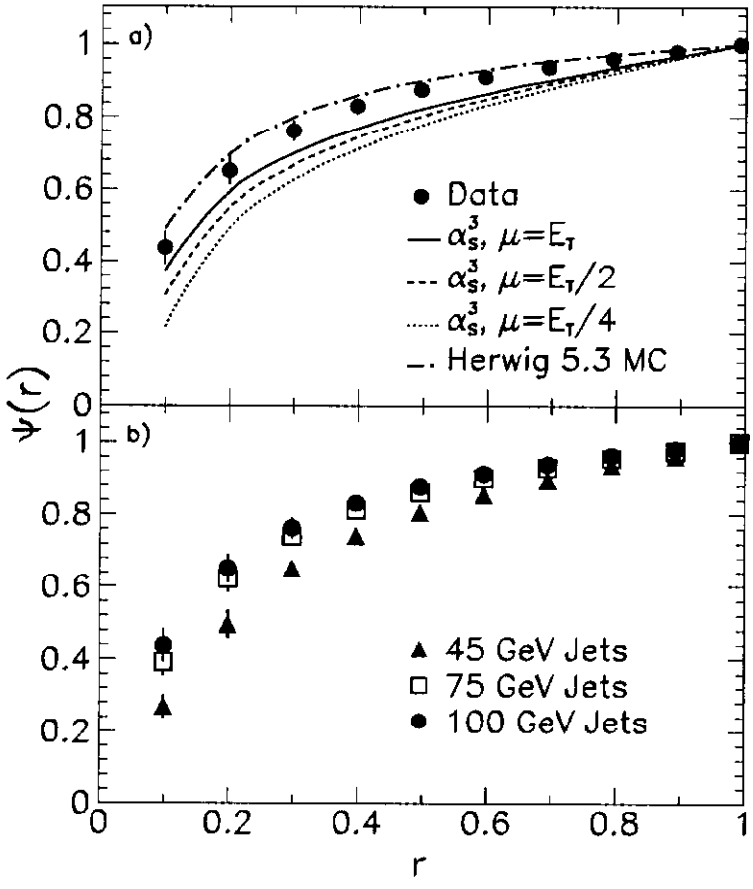
a)
b)
Data
α_s^3, $\mu=E_T$
α_s^3, $\mu=E_T/2$
α_s^3, $\mu=E_T/4$
Herwig 5.3 MC
45 GeV Jets
75 GeV Jets
100 GeV Jets
$\Psi(r)$
r
0
0.2
0.4
0.6
0.8
1

Figure 2.

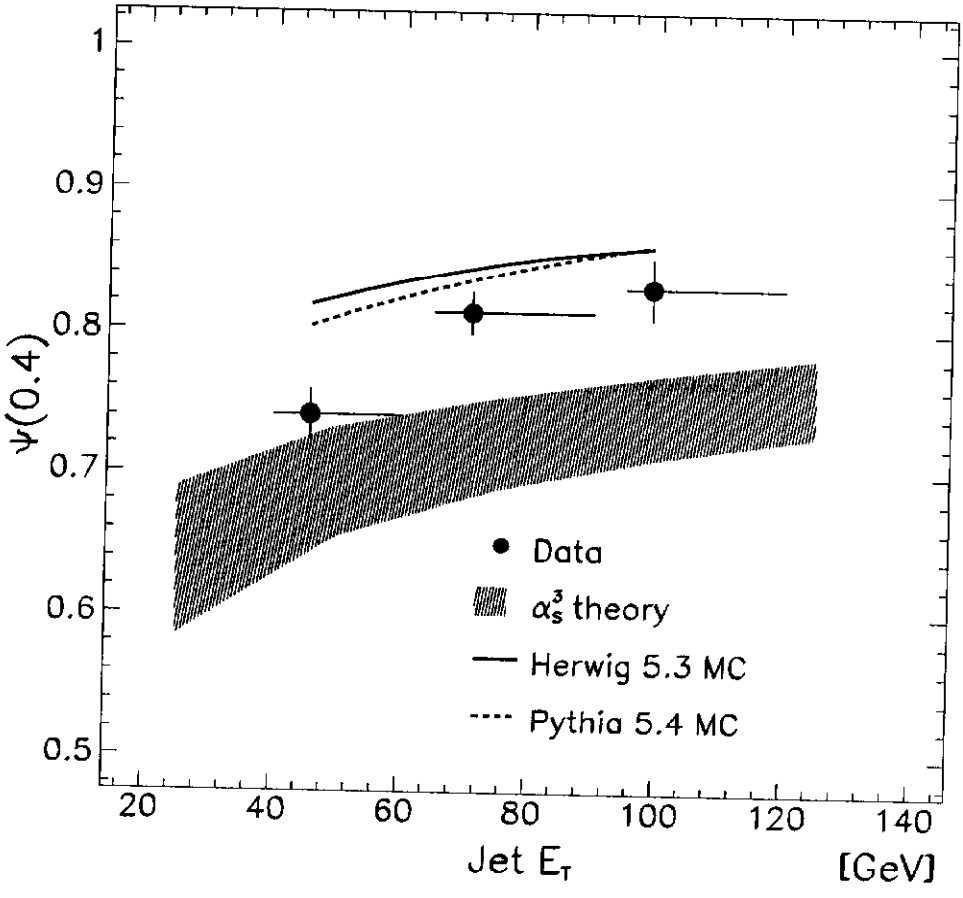
1
0.9
0.8
0.7
0.6
0.5
Ψ(0.4)
20
40
60
80
100
120
140
Jet E_T [GeV]
Data
α_s^3 theory
Herwig 5.3 MC
Pythia 5.4 MC